Journal of Applied Polymer Science

Evaluation of Hydroxyl Terminated Polybutadiene-Isophorone Diisocyanate Gel Formation During Crosslinking Process

Nicolas Ducruet,[1,2] Luc Delmotte,[1] Gautier Schrodj,[1] Francine Stankiewicz,[2] Nancy Desgardin,[2] Marie-France Vallat,[1] Bassel Haidar[1]

[1]Institut de Sciences des Matériaux de Mulhouse (LRC 7228 CNRS – UHA) 15, rue Jean Starcky BP 2488 68057 Mulhouse Cedex France

[2]SME (groupe Safran), Centre de Recherches du Bouchet 9, rue Lavoisier 91710 Vert le Petit France

Correspondence to: B. Haidar (E-mail: bassel.haidar@uha.fr)

ABSTRACT: Crosslinking reaction of hydroxyl-terminated polybutadiene (HTPB)/isophorone di-isocyanate (IPDI) was monitored by infrared spectroscopy, dynamic mechanical analysis (DMA), swelling measurements, and by relaxation time (T_2) measurements obtained by low-field NMR technique. Chemical reaction monitored by FTIR shows that urethane bonds were predominantly formed throughout the whole reaction period while DMA and swelling became only effective once the three-dimensional network was formed. NMR results allow differentiating between relaxation-processes associated with different fractions of the reactants in the mixture prior to the network formation. The most important finding in this study is that two of the relaxation processes were found to decline whereas a new fraction with a short relaxation time which emerged specifically at an early stage of reaction and progressed along with advancement of the reaction. All results pointed out to a change in the mixture behavior around 30 h of crosslinking reaction at 60°C, reflecting an important restriction in molecules diffusion and mobilities which were attributed to the gel point formation. © 2012 Wiley Periodicals, Inc. J. Appl. Polym. Sci. 000: 000–000, 2012

KEYWORDS: polyurethane; low field-NMR; T_2 relaxation; gel point; crosslinking

Received 22 March 2012; accepted 10 June 2012; published online
DOI: 10.1002/app.38194

INTRODUCTION

Elastomer networks based on polyurethane are extensively used as engineering materials thanks to their mechanical, thermal, water permeability, low temperature resistance, and adhesive properties. One of their important applications is in hydroxyl-terminated polybutadiene (HTPB) composite compounding for energetic materials such as explosives, pyrotechnic, propellants, and liners.[1,2] Properties-control, which depends essentially on the degree of crosslinking, is of great importance in the development of such material. Crosslinking is mainly controlled by the use of the NCO/OH ratio.[3] In addition, the hydroxyl groups in HTPB are actually not restricted to the end-groups, some polyol molecules are often present and the polyol/diol ratio enhances the crosslinking in opposition to chain-extending processes and consequently mechanical properties as well.

Especial attention has been paid to select the most appropriate structure of the isocyanate which should complement the HTPB, its functionality, its reactivity which determine the "pot life" of the mixture and the average molecular weight of HTPB in the mixture. Therefore, the effect of crosslinking agents on the structure and properties of polyurethane has been studied for several reactive molecules such as toluene diisocyanate (TDI), isophorone diisocyanate (3-isocyanatomethyl-3,5,5,-trimethycyclohexyl isocyanate IPDI), and methylene bis(cyclohexylisocyanate) (HMDI).[4] However, isophorone-diisocyanate (IPDI) was found to be more effective since much less reactive than TDI, which was broadly used in previous studies, thus enhancing the pot life and minimizing defects and materials waste.

Although such materials are mostly used as filled networks, and rather as highly filled networks in the case of propellants, the characterization of the unfilled network is essential for optimization of the crosslinking reaction and consequently the material characteristics.

Methods adopted for the determination of the kinetics of gel formation and crosslinking density are based on the assessment of either the physical properties such as swelling, toughness (uniaxial tensile, stress–strain evaluations), thermal properties, DSC,[5] or by direct chemical tracking of the reactants and the

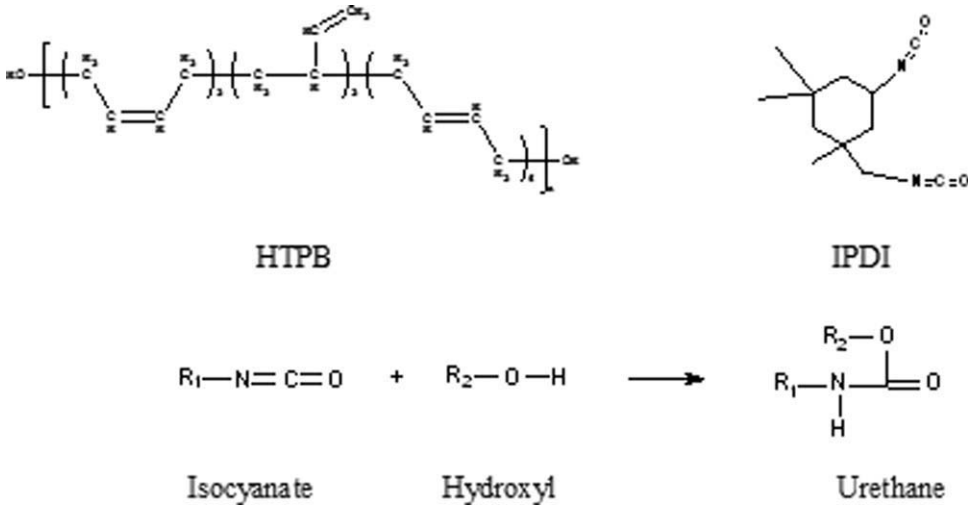

Figure 1. HTPB and IPDI structures and urethane bond formation.

products of the crosslinking reaction using chemical tools such as infrared spectroscopy.[6–8]

^{13}C- and ^{1}H-Nuclear Magnetic Resonance NMR techniques are also routinely used for monitoring chemical changes as a function of reaction time; their performance depends on the intensity of chemical shifts which was improved by using increasingly higher field NMR machines. ^{1}H is the most prevalent NMR nucleus, extensively applied to polymers and generally forms a rather broad line associated with the residual dipolar coupling and restricted mobility of the polymer chains. Moreover, since ^{1}H is an excellent probe for molecular dynamics it was extensively used in monitoring physical changes. However, results obtained through solid- or Hahn-echo's (NMR sequences used in polymer studies) are subject to possible errors and may be contaminated by residual interactions. Such diverse artifacts were usually overcome by finely designed pulse sequences.

In a totally inverse strategy, the new generation of low cost, low field (LF), LF-NMR spectrometer is a flexible analytical tool, developed with the primary objective of "process-monitoring in a quasi industrial environment". A direct analysis of reactive chemical group concentration during chemical reaction is virtually out of the reach for low field NMR. Still, it is naturally adaptable to describe physical states and environments. It is not surprising, then, if low field NMR was rapidly used in spin-diffusion experiments,[9] for fast tacticity analysis on production sites,[10] assessment of rheometry and monitoring the gelation reaction and gel strength,[11,12] for investigation of the glass transition process in the food polymers[13] or for distinction between different polymer phase mobilities by transverse relaxation times (T_2) relaxometry measurements and even to follow expressly the behavior of HTPB and IPDI in the mixture during curing reaction.[14] However here also, solid- or Hahn-echo's may be contaminated by their lack of specificity but remain though largely used in polymer studies. One can successfully take rid of such contamination by more sophisticated sequences[15–17] and investigations are still in progress in this direction in our laboratory but such remedies are inevitably more time/cost consuming and, thus, are contrary to the primary objective of the low-field NMR.

The purpose of this article is to follow the kinetic of HTPB-IPDI crosslinking reaction by classic chemical and physical means, DMA, swelling and FTIR and to compare the results to those obtained with a simple (CPMG sequence) LF-NMR technique in order to assess its relevance as a "process-monitoring in a quasi industrial environment" and particularly for the measurement of crosslinking advancement.

EXPERIMENTAL

Materials Characteristics

Hydroxyl terminated polybutadiene Poly bd® R45 M (hydroxyl value 0.7100 acetyl meq/g) was a commercial grade from Cray Valley USA LLC (PA - Exton) used as received. GPC measurements were carried out by the analysis department of the research center of the SME Company located in Vert-le-Petit, France. The purpose of this measurement is to assess the characteristic of HTPB chains, Figure 1, in terms of molar masses, MW, and functionalities as defined previously by Allard-Breton et al.[18]

HTPB was dissolved in THF, the GPC carrier. Two detectors were used: a Dynamic Light Scattering (DLS) detector to determine the molar mass distribution of HTPB and a UV detector for the assessment of the chains functionalities. Calibration was made with reference to polystyrene samples ranging from 3100 to 18100 g mol^{-1}.

The determination of HTPB chains functionality, Fi, was possible after labeling HTPB hydroxyl groups with a chromophorous molecule, the dinitrobenzoyle chloride (DNBC). Sample was then tested by GPC and UV detector used. From these results we were able to relate the functionality of these chains to their time of elution and so to their molar masses.

Isophorone diisocyanate (IPDI) (Figure 1) is commonly used as a crosslinking agent for HTPB because of its corresponding low crosslinking kinetics as already shown by others.[19] IPDI from Evonik Industries (trade name Vestanat®) of more than 99.5% w/w purity was used as received.

HTPB and IPDI mixtures were prepared by stirring HTPB and IPDI at room temperature for 1 min and then placed in the FTIR, DMA or LF-NMR measurement's cells at 60°C.

HTPB and IPDI were mixed in 91/9 w/w % corresponding to NCO/OH ratio of 1.154, slightly in excess of IPDI compared to the strict stoichiometric ratio in order to ensure a full reaction.

A specific preparation was used for swelling measurements as described later on. Simple HTPB-IPDI mixtures were also prepared as references for NMR investigations.

Infrared Measurements

The measurements were carried out on a Bruker spectrometer; model IFS66/S, with a standard MCT detector. Measurements were performed with 100 scans in middle infrared region with a spectral resolution of 4 cm^{-1}. The sample was studied through transmission technique to allow quantitative measurements. Sample was placed between 2 KBr pellets and then inserted into a heating device. This device was then preheated and placed into the spectrometer and measurements made every 20 min. The NCO consumption was monitored by the decrease of the NCO band at 2260 cm^{-1} that was normalized with reference to the unchanged C—H band at 1420 cm^{-1}.

DMA Measurements

Measurements were carried out on a METRAVIB VA4000 viscoanalyser with an axial analyzer in shear mode and coaxial cylindrical measurement cell. The test was carried out at constant amplitude (20 μm) with a frequency of 10 Hz. The gap between the probe and the cell is 2 mm and the probe is set 15 mm deep into the sample pod.

Sample was conditioned at 60°C for 10 min before measurement. However, the sample being low-viscous liquid at the beginning of crosslinking reaction, measurements were only accurate after a period of 30 h. The complex shear, elastic and viscous moduli, G^*, G', and G'' respectively, were recorded during 416 h.

Swelling Measurements

Just after mixing of the two components, several samples, of ~ 2 g each, were weighed, w_i, then placed in the preheated oven at 60°C at a time considered as t_0 (30 min after mixing at room temperature). At a given time, t_i, one specimen was taken out, placed in toluene (known as a very good solvent of the polymer), weighed after equilibrium in the swollen state, w_s, and then dried and weighed again, w_d. Swelling percentages, $100 \times (w_s - w_d)/w_d$ were determined. These measurements were recorded over 140 h.

Low Field NMR Measurements

Low field NMR apparatus (20 MHz) is supplied by Bruker under the commercial name of Minispec®. The measurement temperature was regulated with ± 0.1 K accuracy and manually checked with a thermocouple.

Sample was placed in a NMR tube and thermostated at 60°C for 30 min before T_2 relaxation time measurements were carried out for 336 h.

The sequence used in this article is a Carr-Purcell-Meiboom-Gill (CPMG) one and consists in multiple spin echoes measurements.[20] The intensity of the generated echo is recorded. A progressive decrease of the intensity with the number of echoes is observed because of the impossible fully refocusing of the magnetization. In liquid and viscous samples as the ones studied here the decrease of echo's intensity can be fitted by a sum of exponential functions as given in eq. (1):

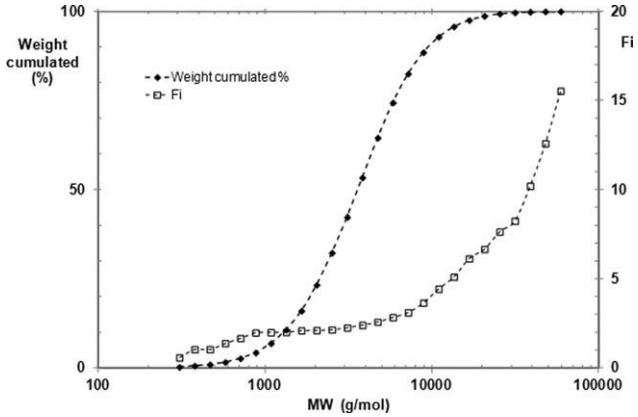

Figure 2. The cumulative fraction MWs (%) and their functionalities (Fi) as a function of MW.

$$M(t) = \sum_i^n f_i \cdot \exp\left(\frac{-t}{T_2(i)}\right) \quad (1)$$

With f_i the proportion of the population i in the sample

$T_2(i)$ the transverse relaxation time of the population i

n the number of relaxation processes.

The fit of the experimental data was done by the SciDavis® software using a normalized Levenberg-Marquardt algorithm.

Between each sequence a recycle delay is applied. During this delay the excited sample returns to its equilibrium state. The recycle delay was chosen equal to 5 s to avoid saturation of the signal between each sequence. The 90° pulse and 180° durations are respectively equal to 2.88 μs and 5.72 μs.

The τ value was chosen equal to 0.1 ms. The train of pulses (n) was chosen to ensure a total decay of the intensity, allowing the measurement of all populations of protons in the sample.

RESULTS AND DISCUSSION

HTPB Characterization

Figure 2 presents the HTPB molecular mass distribution and their functionalities.

The HTPB mean average of number molecular weight is 2900 g/mol. One can notice that the longer the HTPB chains the higher their functional groups content. Beyond a threshold value of functionality equal to 2 which correspond to a rough 70% of the polymer, the functionality increases rapidly but this concerns a small number of chains. The overall average number of functional group per polymer chain remains quite low, 2.2. It is expected, therefore, that HTPB would lead to the formation of a very loose network when crosslinked with a bi-functional isocyanate such as IPDI.

Infrared Measurements

FTIR measurements were made in order to track the kinetic of chemical reaction. Figure 3 shows the *in situ* FTIR spectra

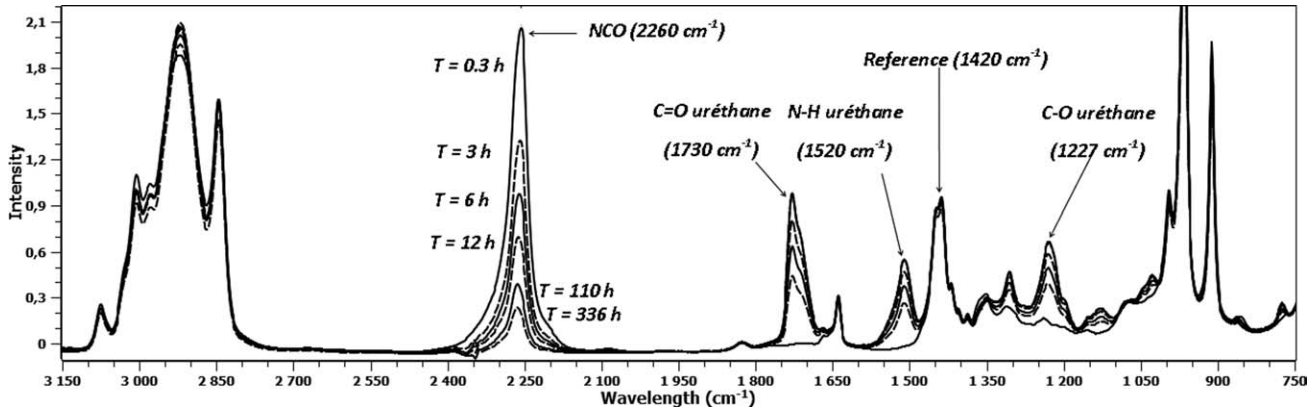

Figure 3. Spectra of the PBHT-IPDI mixture at various indicated times of crosslinking reaction at 60°C.

during the progress of crosslinking reaction of HTPB-IPDI mixture at 60°C.

Several IR bands are clearly evolving during the crosslinking reaction, as shown Figure 3. The formation of the urethane functional groups is specifically related to the decrease of the isocyanate peak and the increase of the carbonyl peak. NCO groups, known to be centered at 2260 cm^{-1}, are mainly converted into urethanes groups[21] as corroborated by the emergence of C=O (1730 cm^{-1}), C—O (1227 cm^{-1}), and N—H (1520 cm^{-1}) bonds. The kinetic of NCO conversion was studied by following the normalized intensities, $(I_{it}/I_{ref})/(I_{i0}/I_{ref})$ (where I_{it} and I_{i0} are the intensities of the 2260 cm^{-1} band at crosslinking reaction time t and t_0 respectively, and I_{ref} is the intensity of the 1420 cm^{-1} band). Results are shown on Figure 4 as a function of crosslinking duration, t. It is remarkable from this figure that after 336 h, 10% of NCO functional groups remain yet unreacted.

Similarly, the three urethane bonds were found to follow the same evolution. As an example, the intensity of C—O bond (1227 cm^{-1}) normalized with reference of the unperturbed band (I_{it}/I_{ref}) at 1420 cm^{-1} is presented Figure 5.

Both kinetics in Figures 4 and 5 follow fairly well a second order kinetic with a R^2 coefficient being superior to 0.99. The kinetic seems to present two different coefficients, as presented eq. (2),

$$I_i = 1 - \left(\frac{I_1^t}{(1 + 2 \cdot I_1^t \cdot k_1 \cdot t)} + \frac{I_2^t}{(1 + 2 \cdot I_2^t \cdot k_2 \cdot t)} \right) \qquad (2)$$

- For NCO bond
  I_1^t is the intensity of the NCO bond at the beginning of the first time domain, $t = 0$ h.
  I_2^t is the intensity of the NCO bond at the beginning of the second time domain, $t = 30$ h.
- For urethane bonds
  I_1^t is the intensity of the CO bond at the end of the first time domain, $t = 30$ h.
  I_2^t is the intensity of the C—O bond at the end of the second time domain, $t = 336$ h.

The values of k factors change around 70% of NCO conversion, corresponding to a crosslinking duration of ≈ 30 h. k values were obtained by fitting the intensities of various peaks using the kinetics of equation given in SciDavis®. k_1 and k_2 correspond to the values at $t < 30$ h and $t > 30$ h domains respectively as shown on Table I.

It can be considered that NCO conversion leads mainly to urethane formation as reflected by similar order of magnitude of k values. The kinetic change occurred around 30 h of reaction (about 70% of NCO conversion). It is most likely due to a corresponding modification of the reaction medium that may be associated with a three-dimensional gel formation.

DMA Measurements

Elastic and loss moduli, G' and G'', are presented in Figure 6 as a function of the crosslinking time. As expected, the reaction leads to an increase of the elastic modulus associated with a

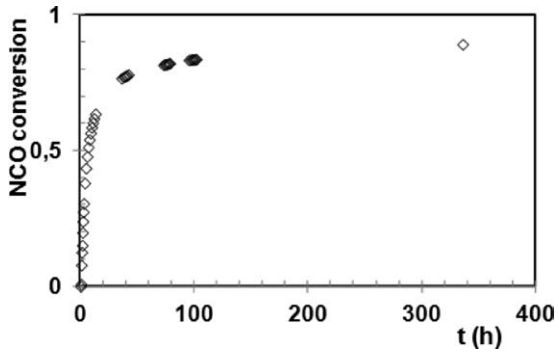

Figure 4. NCO conversion during crosslinking process.

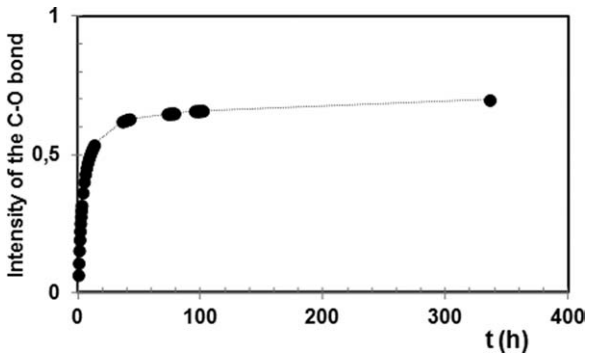

Figure 5. The kinetic of urethane formation of C—O bond at 1227 cm^{-1}.

Table I. k Factors of eq. (3) During Crosslinking Reaction

Domain		NCO	C=O	N—H	C—O
$1 : t < 30$ h	k_1	0.13	0.09	0.153	0.14
$2 : t > 30$ h	k_2	0.0002	0.0003	0.00002	0.00009

much weaker but steady increase of G''. We note however the low values of G', few kPa, a clear indication of the loose structure of the network. A limited extrapolation of G' values to shorter time leads to a G'-G'' crossover point at a reaction time of 27 h, which can be considered as the "mechanical" gel point, t_g, as a result of the crosslinking process.

Swelling Measurements

Swelling measurements results at equilibium are presented in Figure 7.

It is clear that the swelling ratio decreases quite linearly with increasing crosslinking time in a logarithmic scale which may be attributed to the fact that crosslinking process is controlled by a diffusion process. Swelling ratio remains however quite high, ~500%, after 336 h of reaction, reflecting a low crosslinking density. The gel point, defined as the instance when the first macroscopic three-dimensional network is formed, is hardly sizeable by swelling measurement. In fact swelling can be actually effective only when the network becomes consistent enough to hold the weight of the solvent it absorbs in addition to its own weight. Such conditions need a quite advanced crosslinked network. Therefore, the first measurable specimen at 60 h of crosslinking time is presumably well above the strict definition of the "effective" gel-point.

Low Field NMR Measurements

LF-NMR measurements were carried out at 60°C first on pure reactants, IPDI and HTPB, then on their simple unreacted mixture before examining the mixture during the actual crosslinking reaction time.

Pure Molecules

In the case of simple monodisperse molecule such as isocyanate, the decrease of magnetization intensity exhibits a single proton

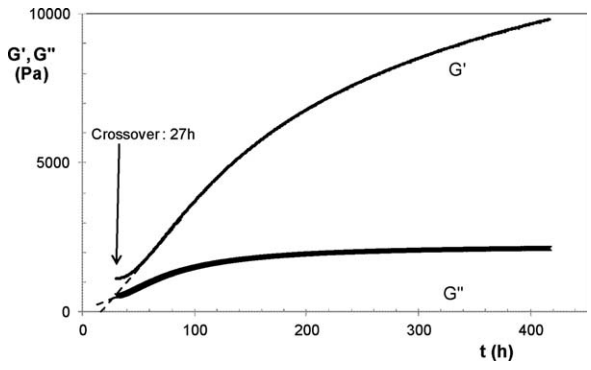

Figure 6. DMA results during crosslinking reaction of HTPB-IPDI mixture.

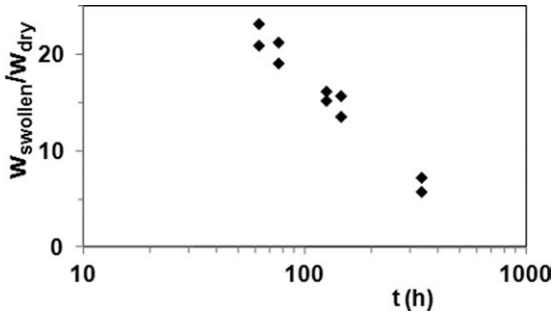

Figure 7. Swelling ratio of HTPB and IPDI mixture at various time of crosslinking reaction.

population, ($n = 1$ in eq. (1)), of the longest relaxation time T_2 centered at ≈560 ms, Table II.

In case of polymers, magnetization decay is known to be much more complex than that of simple molecules.[22,23] In various polymers such as polydimethylsiloxane rubber,[24,25] polybutadiene rubber,[26] and butyl rubber,[27] the global magnetization decay was composed of 2 or 3 relaxation times in order to fit correctly the CPMG data ($R^2 > 0.999$).

For a good fit of HTPB magnetization decay, shown on Figure 8, n was found equal to 3, reflecting the presence of three different proton populations, with T_2 increasing from 45 to 97 and 260 ms and population fractions equal to 33, 58 and 8 % respectively, Table II.

It is not an easy task to attribute each relaxation time to distinct physical significance. In crosslinked 1,4 *cis* polybutadiene, Simon et al.[28,29] stated that different relaxation times measured similarly by the CPMG sequence are related to the contrasts of different mobilities existing in this system. Such diversity of mobility corresponds to diversity of polybutadiene chains morphology (crosslinked, dangled, or sol). The short T_2 were attributed to the influence of physically or chemically crosslinked chains, medium T_2 representing chains ends or defects effects and the long relaxation times corresponding to very mobile molecules as in the sol fraction. The molecular weight between entanglements, M_e, of cis-trans polybutadiene is indicated in the literatures as equal to 4600 g/mol[30,31] that we consider as the M_e value of our polymer despite the presence of OH groups in chain-ends. Accordingly, GPC results reported on Figure 2 shows that the proportion of entangled chains in the HTPB is of about 36%. This value may be compared to the proportion of the short relaxation time population, $T_2 = 45$ ms, in Table II which is about 33%. The accordance between the two values suggests that the short relaxation time fraction observed by NMR may be attributed to the physically

Table II. Proportion of Each Population in Pure IPDI and HTPB at 60°C

	Short		Medium		Long	
	%	T_{2S} (ms)	%	T_{2M} (ms)	%	T_{2L} (ms)
HTPB	33	45	58	97	8	260
IPDI	/	/	/	/	100	560

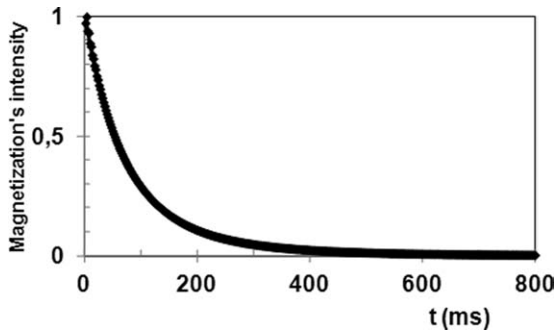

Figure 8. Magnetization decay of pure HTPB measured by CPMG sequence at 60°C (◆) and the perfectly superposed fit using three relaxation times (–).

crosslinked (entangled) chains of HTPB. Under this figure, the medium fraction would be associated with $M_n < M_e$ and the 8% of the polymer having a long relaxation time, 260 ms, could be related to the HTPB oligomers and/or nonpolymeric materials such as additives and antioxidant and will be considered as negligible in a first approximation in the mixture.

Mixtures of HTPB and IPDI

When different ratios of HTPB/IPDI mixtures were examined by CPMG LF-NMR, good fits of the data were achieved by introducing three components.

Figure 9 shows the corresponding fractions (A) and relaxation time (B) of the three populations as a function of the %w HTPB.

Considering the results obtained for pure components, Table II, one would be tempted to attribute the longer T_2 fraction in the mixtures to the IPDI molecules and the the two shorter T_2 fractions to the polymer. It appears from Figure 9(A) that the amount of the more mobile protons (long T_2 population) decreases nearly in a linear relationship whereas the contributions of the two other populations increase also linearly over the whole domain of HTPB concentration; the sum of the amount of the three populations is very close to 100 which prove the pertinency of the three componends representation in the present case. Such an evolution suggests that the long T_2 population can be associated with IPDI almost exclusively in first approximation; its perfect linear evolution, with a slope very close to one, shows that this population behaves in the mixture as a whole and remains "quantitatively" unaffected by its neighbours. Similarly, the two shorter T_2 populations can be associated with HTPB; the sum of the two fractions is also equal to the whole amount of 1H in the polymer for all mixtures.

The mobilities of the two components, as reflected by T_2 relaxation time in Figure 9(B), are highly affected by their environments. The three relaxation times decrease fairly linearly with the amount of HTPB in the mixture. This decrease in T_2 results from the environmental change of each proton fraction which is presumably due to the increase of the medium viscosity.

HTPB-IPDI Crosslinking Reaction

The evolution of 91/9 wt % of HTPB and IPDI mixture after 2 min of mixing was followed under crosslinking conditions, at 60°C for 336 h. Results at the early stage of the reaction, up to 3–4 h as shown in Figure 10, can, like in simple mixtures, be fitted with three relaxation processes. The three relaxation times decrease linearly with a logarithmic scale of the crosslinking time, t, as shown in Figure 10. We observe a clear alteration of the process after about 50 h of crosslinking, the decrease of T_2's is highly reduced.

But the most noticeable observation of these results is a progressive rise of a new population (pop N) as shown on Figure 10. It has an even shorter relaxation time (≈ 6ms) than all fractions observed in the mixture which decreases further with the development of the crosslinked network in a qualitatively similar pattern as the three fractions previously discussed, Figure 10. This new population is obviously driven by the formation of chemical network; therefore, it may be taken as a direct indicator to monitor the progression of crosslinking reaction under real productions conditions.

The sums of the different fractions are acceptably close 100% in general as seen in Figure 11, although longer crosslinking times suffer a slight increase of the reconstitution sums above 100%. The quantitative evolutions of the three "original" populations are quite peculiar as shown in the same Figure 11. At the beginning of the crosslinking process for about 2 h, T_2 values are

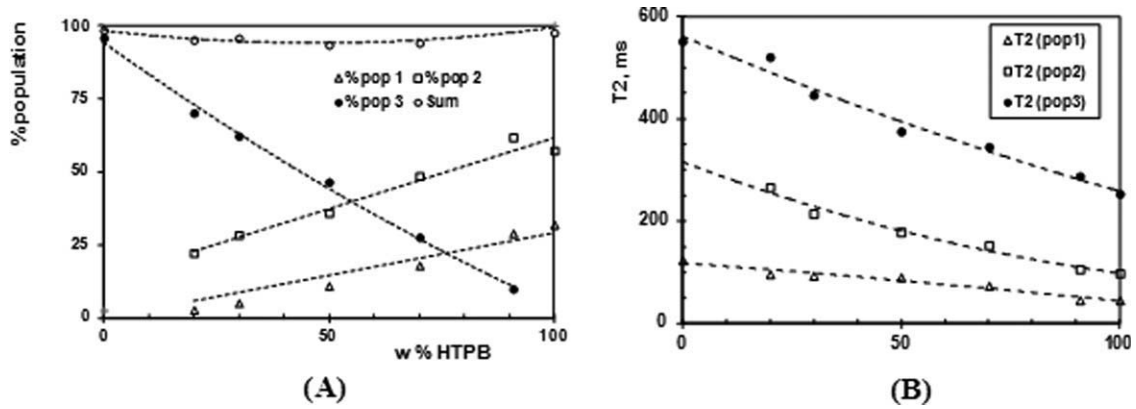

Figure 9. Proportion of short (Pop 1) medium (Pop 2) and long (Pop 3) populations (A) and their relaxation times (B) as a function of mass ratios of HTPB in HTPB-IPDI mixtures.

quite stable. For longer times, while both the long (T_{2L}) and medium (T_{2M}) population fractions (attributed, in the mixture, essentially to the IPDI and to short HTPB polymer chains, $M < M_e$, respectively) decrease rapidly with crosslinking time whereas the short (T_{2S}) population fraction (attributed, in the mixture, to entangled long chains, $M > M_e$) increases during the first 10 h then, stabilizes for longer times. The two decreasing populations should presumably be associated with the depletion process of the reactants during the chemical reaction; i.e., IPDI for T_{2L}, and short HTPB for T_{2M} since short chains are the most reactive ones. At an early stage of the reaction, < 20 h, the chain-extension process is the most active, leading to the increase of the T_{2S} population associated with entangled chains, $M < M_e$, which reaches a plateau (after about 15 h of crosslinking reaction. Worth mentioning here that the sum of these three populations is constant during the first hours of reaction, than decreases in a monotone way as long as the crosslinking reaction advances.

The merging population, $T_{2N,}$ appears clearly after 4 h of crosslinking and continues to progress as long as the crosslinking reaction progresses. The fairly good linear evolution of the crosslinking process as a function of log-time indicates that crosslinking reaction is basically governed by a diffusion process.

The presence of such a short relaxation time population in a fully crosslinked HTPB-IPDI systems was mentioned in the literature, the proportion we observed after 336 h of reaction is in good agreement with the 1 ms value obtained by Mowery et al.[32] However, the present results show for the first time that a population, T_{2N}, can be considered as exclusively related to the forming "network," thus, it can be used as a specific indicator in a rapid monitoring of the crosslinking reaction in a practical production environment. Furthermore, crosslinking reaction appears to proceed by urethane formation reaction in two steps, the first consists essentially on chain extension reaction, only in a second step network formation starts indeed. It is important to notice that this network initiating around 4h reaction is physically distinguishable from the gel point where a macroscopic tridimensional network is formed. All 3 methods of material characterization,

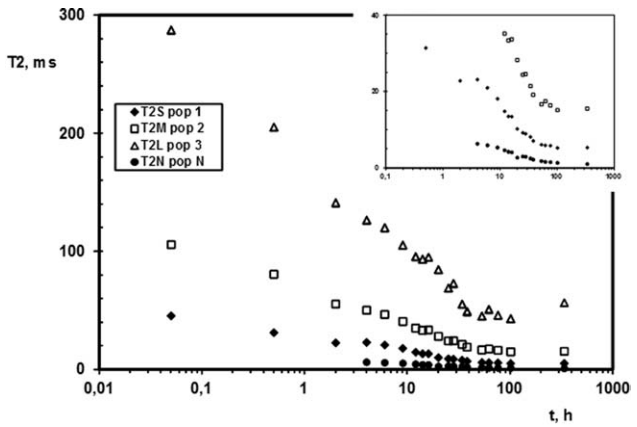

Figure 10. The relaxation times of the various populations as a function of crosslinking time during crosslinking reaction of HTPB-IPDI stoichiometric mixture (insert is a zoom at short times–symbols are identical for both figures).

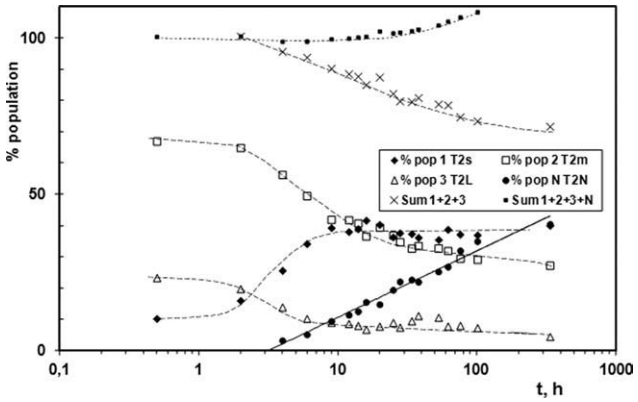

Figure 11. Quantitative evolution of the four T_2 populations presented in Figure 10 and their sums as presented in the legend.

FTIR, DMA, and LF-NMR seem to point accurately at the same gel point in contrast with swelling measurements that need gelification process to progress further to higher crosslinking-time (60 h) in order to produce a network able to handle the amount of solvent it absorbs during the swelling process.

CONCLUSIONS

The monitoring of HTPB/IPDI crosslinking reaction by FTIR spectroscopy, swelling, and DMA measurements points out that the kinetic of NCO conversion produced mainly urethane bonds. The formation of a three dimensional network identified by a characteristic latent-period known as the gel-point corresponds to the deceleration of the chemical reaction governed by diffusion process. Gel point value was found to depend on the technique used for its determination with an increase in the order FTIR = DMA = NMR < swelling. This can be attributed to the differences in sensitivities for each measurement approach and to the scale at which it acts.

T_2 measurements by LF-NMR appeared to be a handy tool to monitor crosslinking reaction. It identifies several fractions of protons with T_2 ranging from several hundreds to few ms, associated with molecules and segment which differ either in nature, physical restriction, or in molecular weight. The identification of these fractions is not always straightforward. The most remarkable observation is that related to a new T_2 population (few ms) which emerges after 4 h of reaction and steadily increases in proportion along with the crosslinking reaction to become the main population in the sample after 336 h of reaction. The appearance of this fraction marks the initiation step of network-formation after a quasi exclusive chain-extension step. In parallel the relaxation time of this fraction decreases. The presence and detection of this population can be used, qualitatively and quantitatively, as a handy and fast indicator in the properties- and pot life-control of HTPB-IPDI-based composites.

REFERENCES

1. Krishnan, S.; Swami, R. D. *Defence Sci. J.* **1998,** *48*, 211.
2. Van der Heijden, A. E. D. M.; Leeuwenburgh, A. B. *Combust. Flame* **2009,** *156*, 1359.

3. Sekkar, V.; Bhagawan, S. S.; Prabhakaran, N.; Rama Rao, M.; Ninan, K. N. *Polymer* **2000,** *41*, 6773.
4. Sekkar, V.; Gopalakrishnan, S.; Ambika Devi, K. *Eur. Polym. J.* **2003,** *39*, 1281.
5. Desai, S.; Thakore, I. M.; Sarawade, B. D.; Devi, S. *Eur. Polym. J.* **2000,** *36*, 711.
6. Burel, F.; Feldman, A.; Bunel, C. *Polymer* **2005,** *46*, 15.
7. Lapprand, A.; Boisson, F.; Delolme, F.; Méchin, F.; Pascault, J. P. *Polym. Degrad. Stab.* **2005,** *90*, 363.
8. Kopusov, L. L.; Zharkov, V. V. *Zhurnal Prikladnoi Spektroskopii* **1966,** *5*, 125.
9. Hedesiu, C.; Demco, D.E.; Kleppinger, R.; Adams Buda, A.; Blümich, B.; Remerie, K.; Litvinov, V. M. *Polymer* **2007,** *48*, 763.
10. Litvinov, V. M.; Soliman, M. *Polymer* **2005,** *46*, 3077.
11. Laura, R. Z.; Kantzas, M. F. A. *SPE Reservoir Eval. Eng.* **2008,** *11*, 439.
12. Abdollah, O.; Ayret, M.; Carlos, M.; Stapf, S. *Thermochim. Acta* **2011,** *516*, 52.
13. Ruan, R. R.; Long, Z. Z.; Song, A. J.; Chen, P. L. *Food Sci. Technol.* **1998,** *31*, 516.
14. Hailu, K.; Guthausen, G.; Becker, W.; Köenig, A.; Bendfeld, A.; Geissler, E. *Polym. Test.* **2010,** *29*, 513.
15. Papon, A.; Saalwächter, K.; Schaler, K.; Guy, G.; Lequeux, F.; Montes H. *Macromolecules* **2011,** *44*, 913.
16. Chasse, W.; Valentin, J. L.; Genesky, G. D.; Cohen, C.; Saalwachter, K. *J. Chem. Phys.* **2011,** *134*, 044907-1.
17. Cohen Addad, J. P. *Prog. NMR Spec.* **1993,** *25*, 1.
18. Allard-Breton, B.; Audenaert, M.; Pham, Q. T. *Macromol. Chem. Phys.* **1996,** *197*, 1651.
19. Sekkar, V.; Venkatachalam, S.; Ninan, K. N. *Eur. Polym. J.* **2002,** *38*, 169.
20. Meiboom, S.; Gill, P. *Rev. Sci. Instrum.* **1958,** *29*, 688.
21. Luchkina, L. V.; Askadskii, A. A.; Afonicheva, O. V. *Polym. Sci. Ser. B* **2006,** *48*, 247.
22. Kuhn, W.; Barth, P.; Denner, P.; Müller, R. *Solid State Nucl. Magn. Reson.* **1996,** *6*, 295.
23. Borgia, G. C.; Fantazzini, P.; Ferrando, A.; Maddinelli, G. *Magn. Resonance Imaging* **2001,** *19*, 405.
24. Shim, S. E.; Parr, J. C.; Von Meerwall, E.; Isayev, A. I. *J. Phys. Chem. B* **2002,** *106*, 12072.
25. Shim, S. E.; Isayev, I.; Von Meerwall, E. *J. Polym. Sci. Part B: Polym. Phys.* **2003,** *41*, 454.
26. Oh, J. S.; Isayev, A. I.; Wagler, T.; Rinaldi, P. L.; Von Meerwall, E. *J. Polym. Sci. Part B: Polym. Phys.* **2004,** *42*, 1875.
27. Feng, W.; Isayev, A. I.; von Meerwall, E. *Polymer* **2004,** *45*, 8459.
28. Simon, G.; Baumann, K.; Gronski, W. *Macromolecules* **1992,** *25*, 3624.
29. Simon, G.; Schneider, H.; Häusler, K. G. *Prog. Colloid Polym. Sci.* **1998,** *78*, 30.
30. Boyer, R. F.; Miller, R. L. *Polymer* **1976,** *17*, 925.
31. Boyer, R. F.; Miller, R. L. *Polymer* **1987,** *28*, 399.
32. Mowery, D. M.; Assink, R. A.; Celina, M. *Polymer* **2005,** *46*, 10919.